Directing Integrin-linked Endocytosis of Recombinant AAV Enhances Productive FAK-dependent Transduction

Paul M Kaminsky[1], Nicholas W Keiser[1], Ziying Yan[1,2], Diana CM Lei-Butters[1] and John F Engelhardt[1–3]

[1]Department of Anatomy and Cell Biology, College of Medicine, The University of Iowa, Iowa City, Iowa, USA; [2]Center for Gene Therapy of Cystic Fibrosis and Other Genetic Diseases College of Medicine, The University of Iowa, Iowa City, Iowa, USA; [3]Department of Internal Medicine, College of Medicine, The University of Iowa, Iowa City, Iowa, USA

Recombinant adeno-associated virus (rAAV) is a widely used gene therapy vector. Although a wide range of rAAV serotypes can effectively enter most cell types, their transduction efficiencies (*i.e.*, transgene expression) can vary widely depending on the target cell type. Integrins play important roles as coreceptors for rAAV infection, however, it remains unclear how integrin-dependent and -independent mechanisms of rAAV endocytosis influence the efficiency of intracellular virus processing and ultimately transgene expression. In this study, we examined the contribution of integrin-mediated endocytosis to transduction of fibroblasts by rAAV2. Mn^{++}-induced integrin activation significantly enhanced (~17-fold) the efficiency of rAAV2 transduction, without altering viral binding or endocytosis. rAAV2 subcellular localization studies demonstrated that Mn^{++} promotes increased clustering of rAAV2 on integrins and recruitment of intracellular vinculin (an integrin effector) to sites of rAAV2 binding at the cell surface. Focal adhesion kinase (FAK), a downstream effector of integrin signals, was essential for rAAV2/integrin complex internalization and transduction. These findings support a model whereby integrin activation at the cell surface can redirect rAAV2 toward a FAK-dependent entry pathway that is more productive for cellular transduction. This pathway appears to be conserved for other rAAV serotypes that contain a capsid integrin-binding domain (AAV1 and AAV6).

Received 23 September 2011; accepted 11 December 2011; advance online publication 10 January 2012. doi:10.1038/mt.2011.295

INTRODUCTION

Adeno-associated virus (AAV) is a small, nonpathogenic member of the parvoviridae family widely studied for its potential as an effective gene therapy vehicle. It is well accepted that AAV infection begins by binding a primary receptor (*i.e.*, binding-receptor) followed by interaction with a secondary receptor (*i.e.*, coreceptor) required for initiating endocytosis.[1–5] The most extensively studied serotype, AAV type 2 (AAV2), is known to bind membrane associated heparan sulfate proteoglycans (HSPGs) and utilize a variety of coreceptors, including integrins α5β1,[6] αVβ5,[7] fibroblast growth factor receptor 1,[8] laminin receptor,[9] c-MET,[10] and CD9.[11] Although HSPGs are necessary for AAV binding, the identity and function of the core protein(s) of the primary binding receptor(s) remain unknown. Furthermore, it remains to be determined whether the HSPG is endocytosed with AAV and the coreceptor[3] or whether AAV is transferred to the coreceptor on the plasma membrane before endocytosis.[6] After internalization, AAV traffics through various endosomal compartments wherein AAV escapes into the cytoplasm and enters the nucleus. However, a large population of AAV particles remains in perinuclear vesicles for extended periods of time. Even though this event is unfavorable for gene transfer, wild-type AAV likely maintains a latent, intraendosomal population to await coinfection by a helper virus, an event necessary for the replication of wild-type AAV. Although the process regulating endosomal escape is poorly characterized, it is generally accepted that several distinctive AAV internalization pathways exist, each potentially having a unique efficiency of endosomal escape.[7,12–14] It is hypothesized that these pathways are defined by the coreceptor(s) employed, thus identification of an internalization pathway that avoids endosomal entrapment of AAV would be very beneficial to augment gene transfer. In the current study, we sought to evaluate whether integrin-linked entry pathways for rAAV2 are most effective for transducing fibroblasts.

Integrins α5β1 and αVβ5 belong to a subgroup of eight integrins (αVβ1, αVβ3, αVβ5, αVβ6, αVβ8, α5β1, α8β1, αIIbβ3) that classically bind ligands containing an arginine-glycine-aspartic acid (RGD) amino acid sequence and form focal adhesion complexes. Even though AAV capsid proteins do not contain RGD sequences, the presence of an asparagine–glycine–arginine (NGR) or aspartic acid–glycine–arginine (DGR) sequence is highly conserved (amino acids 511-3 of VP1), with the notable exceptions of AAV5 and AAV11 (**Supplementary Table S1**). Although NGR and DGR sequences have poor binding coefficients for the RGD integrin ligand site, binding studies of small peptides have demonstrated that the aspartic acid or asparagine undergoes spontaneous nonenzymatic deamination to isoaspartic acid (isoD) and the binding constants for these peptides containing an IsoDGR sequence rival that of "RGD" containing peptides.[15–17] Furthermore, the NGR sequence

Correspondence: *John F Engelhardt, Department of Anatomy and Cell Biology, University of Iowa, School of Medicine, 51 Newton Road, Room 1-111 BSB, Iowa City, Iowa 52242, USA. E-mail: john-engelhardt@uiowa.edu*

in the AAV2 capsid has been demonstrated to be essential to α5β1 integrin-mediated internalization[6] and αVβ5 integrin-blocking antibodies prevent efficient internalization of AAV2,[7] suggesting that the NGR sequence can interact with the ligand-binding domain of integrins. Additionally, integrin models of focal adhesion formation maintain conserved, but flexible signaling pathways,[18–20] suggesting that AAV may utilize more than α5β1 and αVβ5 integrins.

Integrins play complex roles in focal adhesions, self-aggregate upon activation, and bidirectionally signal through a variety of pathways.[21–24] In brief, the extracellular domains of inactive integrins are folded with their RGD-binding domains hidden, resulting in a very poor binding coefficient to RDG-containing proteins. After interaction with a ligand, the integrin extends and is stabilized by magnesium ions (Mg^{++}).[22,23] Consequently, the integrin ligand-binding site becomes more accessible and RGD-integrin binding becomes significantly stronger; this mechanism is thought to prevent overactivation by RGD-containing peptides in the extracellular matrix. This can theoretically be a significant barrier to infection by AAVs that used integrins as coreceptors. AAV2 is thought to primarily bind to HSPG on the plasma membrane until it interacts with a coreceptor and is endocytosed. As there are potentially many different coreceptors on the surface of target cells, each is likely competing for a limited pool of AAV. Thus, there are two main factors for the interaction with a coreceptor; the quantity of each coreceptor and the binding coefficient with AAV2. We hypothesized that the majority of AAV2 is internalized by competing nonintegrin coreceptors due to poor AAV2–integrin interactions. This is supported by a previous study in which insertion of an RGD repeat domain into the AAV2 capsid increased integrin-mediated transduction and was capable of HSPG-independent infection.[25] One means of promoting integrin–ligand interactions is treatment with manganese (Mn^{++}). Unlike Mg^{++}, which stabilizes the extended integrin conformation, Mn^{++} induces the extension of the integrin without the need for a ligand,[22,24,26] leaving the binding site open for interaction with ligands such as AAV2.

Active integrins also aggregate through intracellular homodimer interactions and extracellular heterodimer interactions. Furthermore, exposed β-integrin cytosolic domains recruit a variety of proteins, such as vinculin, paxillin, talin, and focal adhesion kinase (FAK).[18,21–23,27] In the context of vinculin, this molecule acts to recruit actin to sites of focal adhesion formation.[28] FAK subsequently undergoes intermolecular autophosphorylation at tyrosine 397, recruiting c-Src, Rac1-GEFs, and phosphatidylinositol-3 kinase (PI3K), which further phosphorylate FAK and mediate downstream signaling.[18–20,27] Many of these proteins are kinases that variably phosphorylate other members of the complex, which ultimately results in signaling through several pathways, including PI3K, Rac1/Rho, and MAPK. The pattern of protein recruitment and phosphorylation is determined by a variety of factors including the ligand, involved integrins, integrin-associated proteins, and additional signaling receptors brought into the complex. Interestingly, PI3K and Rac1 signaling were previously demonstrated to be essential to efficient AAV2 internalization, trafficking, and transduction.[7]

Using genetic models and Alexa568-labeled rAAV2, we examined the transduction efficiency and trafficking of rAAV2 internalized by integrin-linked endocytosis. We found that treatment with Mn^{++} enhanced rAAV2 transduction of fibroblasts without altering the efficiency of internalization of virions. Furthermore, Mn^{++} treatment increased the size of rAAV clusters associated with α5 integrin on the cell surface and enhanced colocalization with the integrin effecter vinculin, suggesting that Mn^{++} promotes AAV2–integrin interactions. Lastly, we found that FAK is essential for integrin-linked rAAV2 transduction, and in the absence of FAK, Mn^{++}-induced clustering of rAAV2 failed to internalize. Our studies indicate that integrin-linked endocytosis is a highly efficient transduction pathway requiring FAK for endocytosis.

RESULTS

Integrin activation by Mn^{++} enhances rAAV2 transduction of primary fibroblasts

It is widely accepted that rAAV2 transduction of fibroblasts is extremely poor due to intracellular barriers that limit its efficient movement to the nucleus.[29] By contrast, HeLa cells, which have been shown to primarily utilize integrin-dependent mechanisms of rAAV2 uptake,[7] have 100-fold higher levels of transduction following infection by rAAV2-luciferase virus as compared to primary mouse embryonic fibroblasts (PMEFs; **Figure 1a**). These differences in transduction between these two cell types occur despite equivalent amounts of bound and internalized virus following a 2-hour infection (**Figure 1a**).

AAV2 is thought to primarily bind to HSPG before interacting with a coreceptor and endocytosis. HeLa cells highly express integrins on their cell surface and rAAV2 has been shown to primarily use these molecules as coreceptors.[7] Mouse embryonic fibroblasts (MEFs) also highly express integrins,[30] but additionally express other potential rAAV2 coreceptors such as FGFR-1,[8] c-MET,[10] CD9,[11] and laminin receptor.[9] Therefore, we hypothesized that coreceptors present on the plasma membrane of PMEFs compete for surface-bound AAV and that the dominant coreceptor entry pathway was inefficient at productively processing intracellular rAAV2 for transduction. Furthermore, we hypothesized that an integrin-linked pathway for rAAV2 infection of PMEFs would be most efficient, as in HeLa cells,[7] if sufficient activation of integrins could be achieved at the time of infection. To this end, PMEFs were infected with AAV2-luciferase for 2 hours in the presence of Mn^{++}, which is known to partially activate integrins. Consistent with our hypothesis that integrin-mediated internalization of AAV2 is more efficient at productively processing rAAV2 following endocytosis than competing coreceptors, we observed a 17-fold enhancement of PMEF rAAV2 transduction in the presence of Mn^{++} (**Figure 1b**). Furthermore, this increase in transduction was partially blocked by the integrin-ligand peptide Arg-Gly-Asp-Ser (RGDS) (**Figure 1c**), supporting a functional role for integrins in the process of Mn^{++}-enhanced transduction. Due to the already high level of integrin-dependent transduction of HeLa cells,[7] Mn^{++} only marginally enhanced rAAV2 transduction of HeLa cells (two- to threefold), as anticipated (data not shown).

Mn^{++}-dependent enhancement of rAAV2 transduction in PMEFs is not mediated by increased internalization or binding

Manganese could enhance AAV2 transduction either by increasing the amount of internalized AAV or by altering the efficiency of

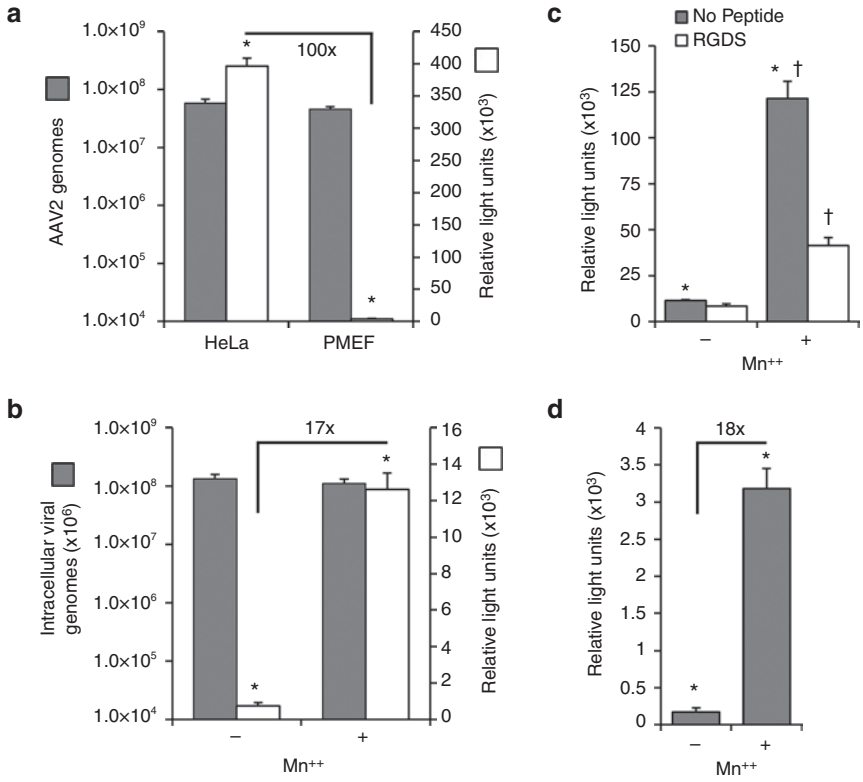

Figure 1 Manganese augments recombinant adeno-associated virus 2 (rAAV2) transduction of primary fibroblasts. (**a**) Transduction of AAV2 is less efficient in C57B6 primary mouse embryonic fibroblasts (PMEF) than HeLa cells. Cells were infected with AAV2-luciferase for 2 hours, after which, internalized/surface-bound AAV2-luciferase was quantified by TaqMan PCR at 2 hours (left axis), and transduction was measured at 24 hours (right axis). (**b**) PMEFs were infected with rAAV2-luciferase in the presence of Mn^{++} for 2 hours, after which virus and Mn^{++} was removed and luciferase activity was quantified 24 hours later (right axis). Internalized viral genomes were quantified after a 2-hour infection with AAV2-luciferase under identical conditions (left axis). (**c**) The integrin-binding peptide Arg-Gly-Asp-Ser (RGDS) inhibits Mn^{++}-induced transduction. AAV2-luciferase transduction was assayed as above in mouse embryonic fibroblasts (MEFs) in the presence of Mn^{++} and/or RGDS peptide. (**d**) Mn^{++} enhances transduction of prebound AAV2-luciferase. AAV2-luciferase was bound to PMEFs at 12 °C for 1 hour to prevent endocytosis. Cells were then washed and shifted to 37 °C and medium-containing Mn^{++} was added for 2 hours. Medium was then exchanged to remove Mn^{++} and luciferase activity was quantified 24 hours later. Values represent the mean ± SEM for $N = 6$ independent infections. Asterisks mark significant differences as assessed by a two-tailed Student's *t*-test ($P < 0.0001$). Fold changes are also marked for selected comparisons.

downstream postendocytic processing of the virus. In order to test whether Mn^{++} increases total AAV endocytosis, intracellular AAV genomes were quantified after a 2-hour infection. Results from these studies demonstrated that the quantity of intracellular genomes was not significantly altered by Mn^{++} treatment at the time of infection (**Figure 1b**). Using a second approach, rAAV2 was cold-bound to PMEFs before treatment with Mn^{++} to ensure that the quantity of AAV available for endocytosis was identical. Similar to our results from a 2-hour pulse infection at 37 °C, transduction of prebound rAAV2 was enhanced 19-fold by Mn^{++}, confirming that the effect is not mediated through increased viral binding or endocytosis (**Figure 1d**). To demonstrate that Mn^{++} does not increase the retention of surface-bound rAAV2, MEFs were prebound with rAAV2 at 12 °C to prevent endocytosis, washed to remove excess virus, and then shifted to 37 °C for 1 hour in the presence or absence of Mn^{++}. The quantity of viral surface-bound and internalized rAAV2 genomes was found to be no different from the initial quantity of bound rAAV2, suggesting that Mn^{++} does not influence the stability of rAAV2 binding to the cell surface (**Supplementary Figure S1**). Additionally, treatment with heparin (1 mg/l) completely inhibited rAAV2 transduction in control and Mn^{++}-treated MEFs, confirming that rAAV2 must bind to HSPGs before engaging a coreceptor under both conditions (**Supplementary Figure S2**). Together, these experiments demonstrate that Mn^{++} acts downstream of rAAV2 binding to HSPGs and does not increase the total amount of internalized virus.

Mn^{++} promotes increased clustering of rAAV2 on integrins and recruits intracellular vinculin

To better understand how Mn^{++} treatment might be altering the dynamics of rAAV2 infection of PMEFs, we first performed localization experiments with Alexa568-rAAV2 as various times postinfection in the presence and absence of Mn^{++}. We noted that consistent Mn^{++}-induced changes in the organization of rAAV particles were observed by 1 hour postinfection (**Figure 2a–b**). Treatment with Mn^{++} increased the size and intensity of Alexa568-rAAV2 aggregates by ~2.5 fold (**Figure 2c**), a number that likely underestimates the difference since most rAAV2 particles are not visible in the absence of Mn^{++}. This is clearly evident in confocal photomicrographs taken at higher thresholds, where abundant rAAV2 clusters could be visualized in Mn^{++} treated, but not untreated cultures (**Figure 2a,b** middle panel), despite equivalent

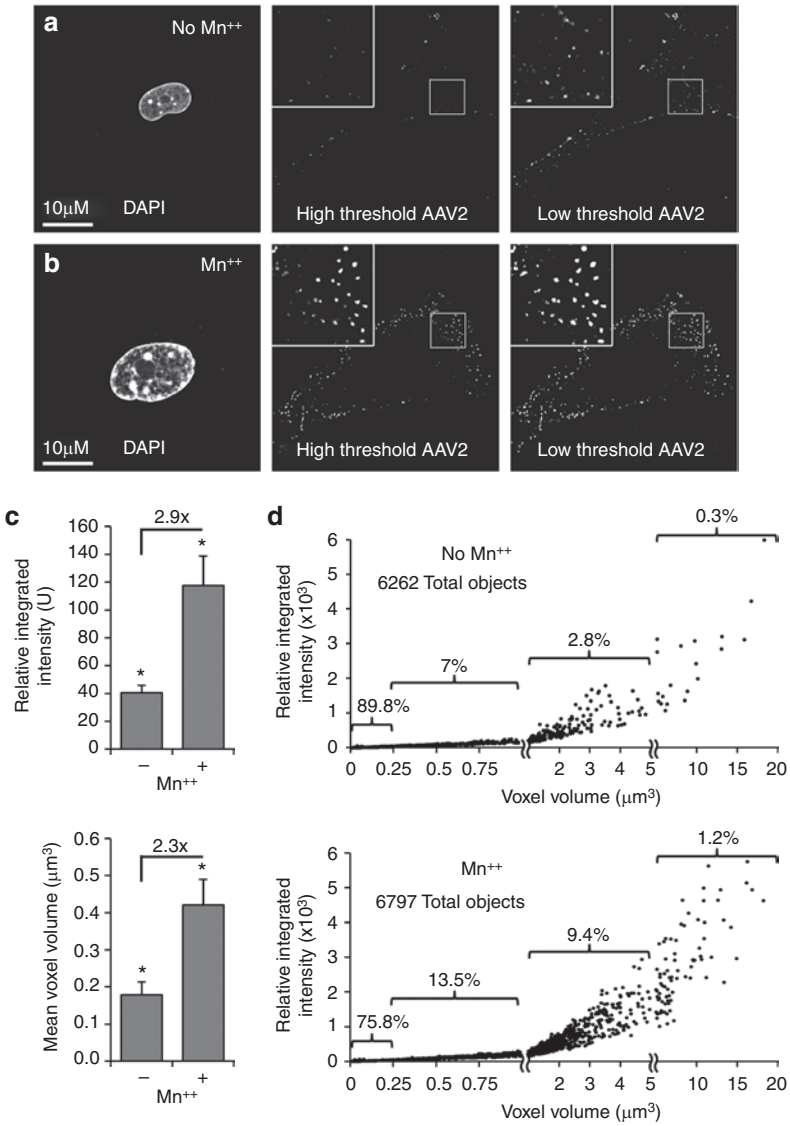

Figure 2 Manganese treatment increases adeno-associated virus (AAV) clustering. (**a**, **b**) Treatment with Mn^{++} increases clustering of rAAV2 and sensitivity of detecting fluorescently labeled virions. Primary mouse embryonic fibroblasts (PMEF) were infected with Alexa Fluor568–rAAV2 (Alexa568-AAV2) for 1 hour with or without Mn^{++} treatment. To accurately image both small and large clusters of rAAV, both low (*i.e.*, high sensitivity) and high (*i.e.*, low sensitivity) thresholds were used when capturing confocal microscopic images. The high threshold was chosen to highlight the increased quantity of large and bright AAV clusters in Mn^{++} treated cells (**b**), while the low threshold panel demonstrates the presence of AAV on untreated cells (**a**). (**c**) The average size and intensity of AAV clusters increases with Mn^{++} treatment. Stacks of confocal images taken through cells infected with Alexa568-rAAV2 for 1 hour, as in (**a**, **b**), were 3D deconvoluted with MetaMorph software. The average intensity and volume of AAV clusters from randomly chosen cells from each condition are shown. Values represent the mean ± SEM of $N = 10$ cells from a representative experiment. Asterisks mark significant differences as assessed by a two-tailed Student's *t*-test ($P < 0.05$ when using averages from each of $N = 10$ cells in the analysis). Fold changes are also marked. (**d**) Effect of Mn^{++} treatment on the distribution of AAV object size as a function of intensity. The average size and intensity of AAV objects used for calculations in (**c**) is presented in an XY scatter plot. The percent of objects contained within selected ranges of AAV cluster size is indicated. For example, in untreated cells, 89.8% of AAV2 objects are between 0 and 0.25 μm^3, which is significantly lower in Mn^{++}-treated cells (75.8%). Statistical comparison between these two groups was significant using at two-tailed Mann–Whitney test ($P < 0.0001$). The number of objects quantified in each panel is indicated.

entry of rAAV2 genomes under the Mn^{++}-treated and -untreated conditions (**Figure 1b**). Morphometric analysis demonstrated that Mn^{++} induces the formation of AAV2 clusters that are larger in size and brighter in fluorescent intensity (**Figure 2d**).

Structural and mutational analysis of the AAV capsid has revealed that the amino acid sequence, NGR, is highly conserved among AAV serotypes and is necessary for interaction with α5β1 integrins.[6] However, there are eight integrin heterodimers theoretically capable of mediating AAV endocytosis (α5β1; αVβ1, αVβ3, αVβ5, αVβ6, αVβ8; α8β1; αIIbβ3) and are variably expressed in many tissues. These integrins play an essential role in bidirectional signaling and the formation of focal adhesions through the recruitment of diverse intracellular proteins, such as vinculin, to the forming focal adhesion. Given that integrin activation would be expected to enhance rAAV2 binding to integrins, we hypothesized that treatment with Mn^{++} would enhance surface

localization of rAAV2 to integrins. To examine integrin recruitment to AAV2 aggregates in the presence of Mn^{++}, we ectopically expressed green fluorescent protein (GFP)-tagged α5 integrin in PMEFs and studied the localization of bound Alexa-labeled rAAV2 at the cell surface. Consistent with our hypothesis, there was extensive colocalization of rAAV2 with α5 integrin in the presence of Mn^{++}; however, we also observed significant colocalization in untreated control cells (**Figure 3a,b**). Despite localization of rAAV2 to α5 integrin-GFP with and without Mn^{++}, the overall abundance of colocalized rAAV2/α5–integrin–GFP complexes was higher in the presence of Mn^{++} due to enhanced rAAV clustering at the membrane, resulting in increased sensitivity of detection by fluorescence microscopy.

Based on these results, we hypothesized that overexpression of α5 integrin-GFP resulted in an abundance of free integrins on the cell surface in the absence and presence of Mn^{++}, and therefore, would mask our ability to use AAV2-integrin colocalization as a functional index for Mn^{++}-induced AAV2 recruitment to

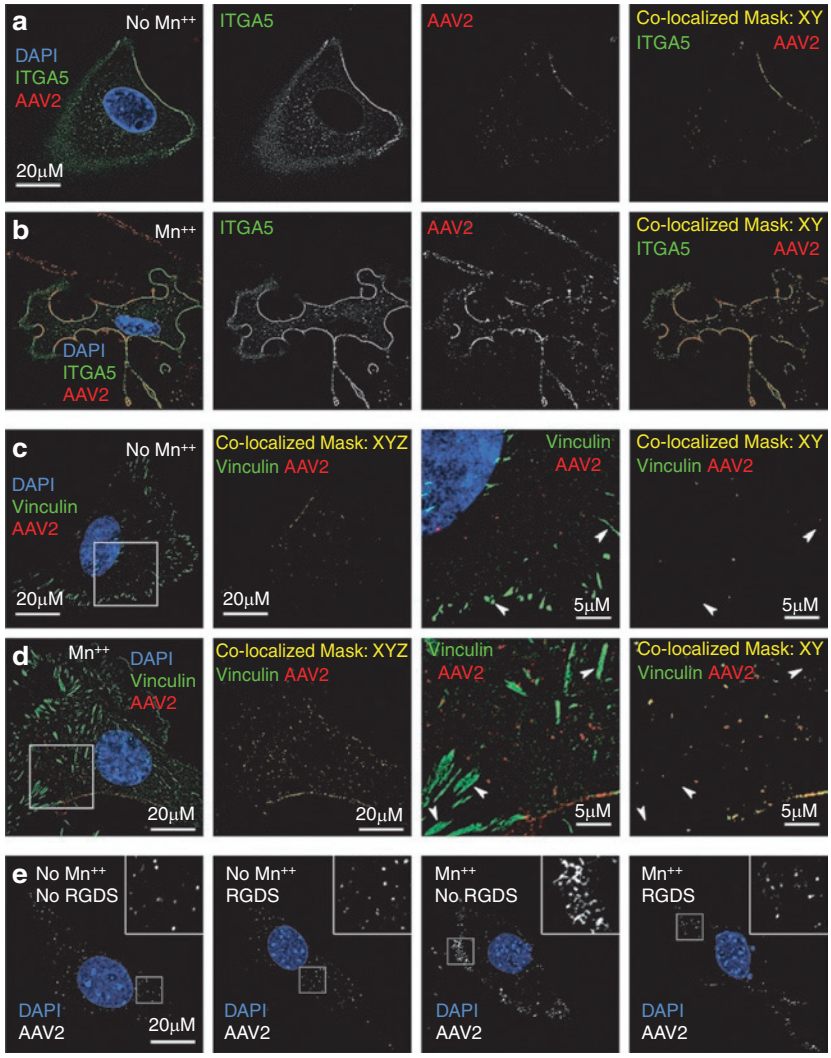

Figure 3 Manganese induces recruitment of intracellular vinculin to sites of recombinant adeno-associated virus 2 (rAAV2) clustering on integrins. (**a**, **b**) AAV colocalization with α5 integrins is increased with Mn^{++} treatment. Primary mouse embryonic fibroblasts (PMEFs) expressing green fluorescent protein (GFP)-tagged α5 integrin were infected with Alexa568-AAV2 for 1 hour with or without Mn^{++} treatment. The images displayed are a single slice from a stack of images that were deconvoluted with Metamorph 3D software. Combined channels are given on the left in color and signal channel images for integrin (green) and rAAV2 (red) are given in black and white in the middle panels. In the right panels labeled "Colocalized Mask," a mask was created using Zeiss LSM software that depicts only colocalized pixels, but does not change the relative intensity of either AAV or integrin staining. A high threshold was used for these images so Mn^{++}-induced clustering could be better appreciated. (**c**, **d**) PMEFs were infected with Alexa568-AAV2 for 1 hour with or without Mn^{++} treatment and stained for vinculin (green). A series of confocal slices were then taken through each cell. The first panel on the left is a slice from the bottom of the cell to depict focal adhesions. These images demonstrate that rAAV2 does not efficiently recruit to focal adhesions that contain vinculin (arrows), even in the presence of Mn^{++}. In the second panel from the left, a colocalization mask was applied to each slice throughout the entire cell and then projected onto a single 2D-image to demonstrate total rAAV2/vinculin colocalization in the cell. The third and fourth panels from the left are magnifications of the area marked in the left panel. "Colocalization mask: XYZ" refers to the Z-stacked masked sections throughout the cell projected into a single 2D image, while "Colocalization mask: XY" refers a mask of a single confocal slice. (**e**) The effect of integrin-binding peptide RGDS on Mn^{++}-induced aggregation of rAAV2. Transformed control MEFs were infected with Alexa568-rAAV2 for 1 hour in the presence of Mn^{++} and Mn^{++} with RGDS peptide. Confocal images are shown with rAAV2 in white and nucleus in blue. Boxed region is enlarged in the inset of each panel.

α5 integrin-GFP. We therefore revised our experimental approach to selectively localize integrin activation at the cellular membrane, hypothesizing that the context (*i.e.*, microenvironment) of integrin activation limits rAAV2 entry into the cell, rather than the overall abundance of integrins on the cell membrane. Vinculin specifically recruits to cellular membranes following integrin activation and this process is known to be important for actin recruitment to forming focal adhesions.[28] We predicted that Mn^{++} would recruit vinculin to sites of rAAV2 binding at the cellular membrane. We also predicted that preformed focal adhesions already containing vinculin would lack rAAV2 binding since RGD-binding site of these integrins would be already occupied. As hypothesized, after a 1-hour continuous infection, Mn^{++} increased the colocalization of Alexa568-AAV2 and vinculin (**Figure 3c,d**), but not at vinculin-containing focal adhesions (**Figure 3c,d**; arrowheads). Furthermore, in the presence of Mn^{++}, both α5 integrin-GFP and vinculin appeared to stay associated with endosomes-containing rAAV2 (**Figure 3b,d**). These findings suggest that clustering of rAAV2 at sites of integrin activation may be important for endocytosis through integrins. In support of this hypothesis, formation of rAAV2 cluters in the presence of Mn^{++} was decreased in the presence of the integrin-binding peptide RGDS (**Figure 3e**). These findings demonstrate that interactions between the virus and integrins are critical for clustering of rAAV2 on the cell surface.

FAK is essential for integrin-linked transduction

We hypothesized that FAK is essential to integrin-linked endocytosis of rAAV2, due to its recognized role in linking integrin activation to downstream effectors Rac1 and PI3K—two proteins essential to rAAV2 endocytosis.[7] To address this hypothesis, rAAV2-luciferase transduction of $FAK^{-/-}$ MEFs was compared to littermate-matched control $FAK^{+/+}$ MEFs (**Figure 4a**). As hypothesized, transduction of $FAK^{+/+}$ cells was significantly greater than that seen in $FAK^{-/-}$ cells. Interestingly, at 20 hours following a 2-hour pulse infection there was only a slight difference in luciferase expression between the two genotypes (twofold), while transduction of $FAK^{+/+}$ cells increased approximately fourfold over

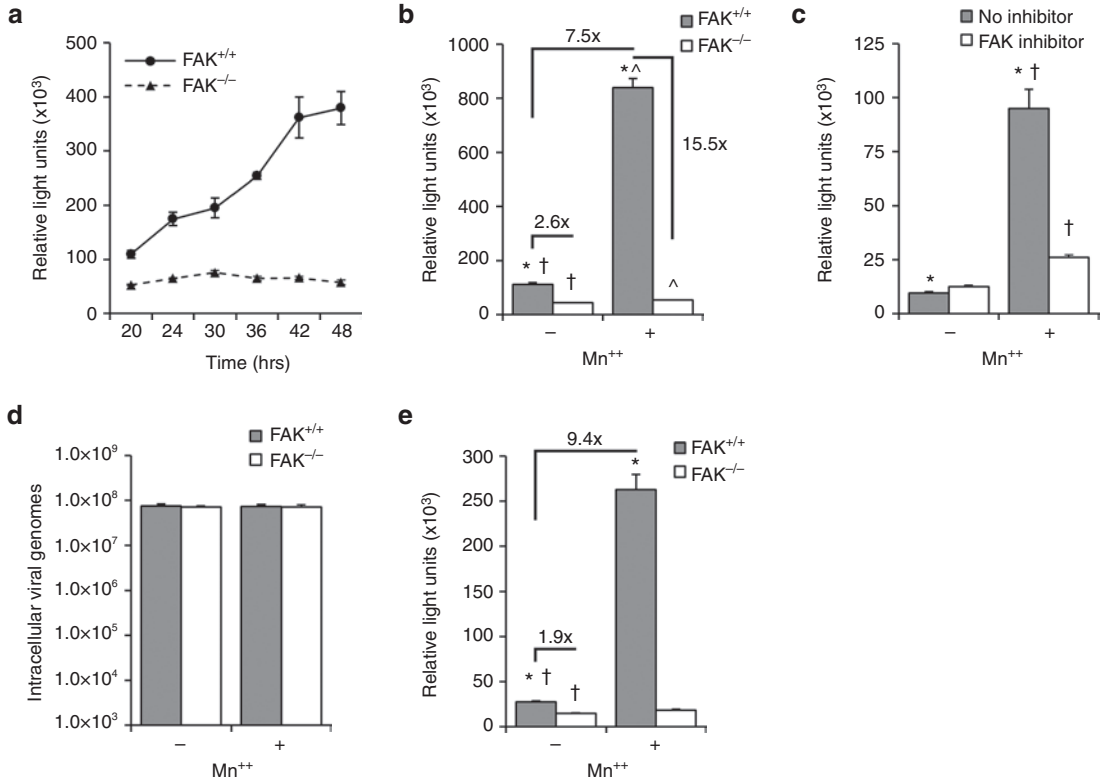

Figure 4 Focal adhesion kinase (FAK) is required for integrin-mediated recombinant adeno-associated virus 2 (rAAV2) transduction. (**a**) Focal adhesion kinase (FAK) is essential for efficient rAAV2 transduction of mouse embryonic fibroblasts (MEFs). $FAK^{+/+}$ and $FAK^{-/-}$ MEFs were infected with AAV2-luciferase and assayed for luciferase expression 20–48 hours after infection. (**b**) Augmentation of rAAV2 transduction by Mn^{++} requires FAK. $FAK^{+/+}$ and $FAK^{-/-}$ MEFs were infected with AAV2-luciferase in the presence or absence of Mn^{++} for 2 hours and luciferase activity was assayed 24 hours later. (**c**) FAK kinase activity is required for Mn^{++} enhancement of AAV2 transduction. $FAK^{+/+}$ MEFs were infected with AAV2 luciferase in the presence or absence of Mn^{++} for 2 hours and the FAK inhibitor PF-00562271 for 24 hours. (**d**) Total AAV2 internalization is not altered by the presence of FAK or Mn^{++}. Fibroblasts were incubated at 37 °C in DMEM containing rAAV2-luciferase with or without Mn^{++} for 1 hour. Extracellular rAAV2 was removed by a 1 mmol/l NaCl wash and trypsinization. Cells were then lysed and the abundance of intracellular rAAV2 genomes was quantified by TaqMan PCR. Controls infected at 4 °C were used to determine the level of membrane-bound virus not removed by the 1 mmol/l NaCl wash and trypsinization (typically <5%). (**e**) Augmentation of rAAV2 transduction by Mn^{++} is independent of AAV2 binding. AAV2-luciferase was bound to $FAK^{+/+}$ and $FAK^{-/-}$ MEFs at 12 °C for 1 hour to prevent endocytosis. Cells were then shifted to 37 °C and medium-containing Mn^{++} was added for 2 hours. Medium was then exchanged to remove Mn^{++} and luciferase activity was quantified 24 hours later. Values in all panels represent the mean ± SEM for $N = 6$ independent infections. *, †, ^mark significant differences as assessed by a two-tailed Student's *t*-test ($P < 0.0001$). Fold changes are also marked for selected comparisons.

the subsequent 20–48-hour period with no change in gene expression in FAK$^{-/-}$ cells—at 48 hours postinfection, transduction was approximately eightfold higher in FAK$^{-/-}$ cells. This finding suggests that rAAV2 transduction through FAK-independent pathways is relatively rapid and unproductive, while FAK-dependent transduction accounts for a majority of rAAV2 transduction.

We hypothesized that if FAK regulates integrin-mediated processing of AAV2, treatment with Mn^{++} would enhance rAAV2 transduction only in the presence of FAK. Consistent with our model, rAAV2-mediated luciferase expression in FAK$^{-/-}$ MEFs was not altered by Mn^{++}, while transduction of FAK competent cells was augmented 7.5-fold by transient 2 hours Mn^{++} treatment at the time of infection (**Figure 4b**). In the presence of Mn^{++}, FAK-deletion reduced transduction at 24 hours by 15.5-fold, but in the absence of Mn^{++}, the FAK-dependency of transduction was significantly lower (2.6-fold). These findings suggest that Mn^{++} increases utilization of a FAK-dependent transduction pathway that more effectively leads to transgene expression. Additionally, pharmacologic inhibition of FAK kinase activity with PF-00562271 blocked Mn^{++}-induced transduction, confirming that the effect of Mn^{++} requires FAK kinase activity (**Figure 4c**). The presence of FAK, or treatment with Mn^{++}, did not significantly alter AAV2 uptake as quantified by TaqMan PCR, demonstrating that AAV2 internalization remains efficient in the absence of FAK (**Figure 4d**). Furthermore, Mn^{++} enhanced transduction of 12°C prebound of AAV2 (9.4-fold) similarly to treatment during infection (**Figure 4e**), demonstrating that Mn^{++} induces a process following viral binding. These findings support the notion that fibroblasts have multiple efficient methods of endocytosis of rAAV2, but that the integrin/FAK-dependent pathway of endocytosis is much more efficient in productive transduction.

FAK is required for integrin-mediated internalization of AAV2

Previous studies from our laboratory have established that integrin-mediated internalization of AAV2 requires PI3K and Rac1.[7] Similarly, studies of focal adhesions have demonstrated that integrin-mediated activation of FAK stimulates PI3K and Rac1 activity. However, there is very little knowledge about pathways of integrin-linked endocytosis. We hypothesized that FAK is required for integrin-linked internalization of rAAV2 and that in the absence of FAK, endocytosis of cell-surface-bound rAAV2 is mediated by alternative secondary coreceptors. To test this model, FAK$^{+/+}$ and FAK$^{-/-}$ MEFs were infected with Alexa568-AAV2 in the presence of Mn^{++} (**Figures 5** and **6**).

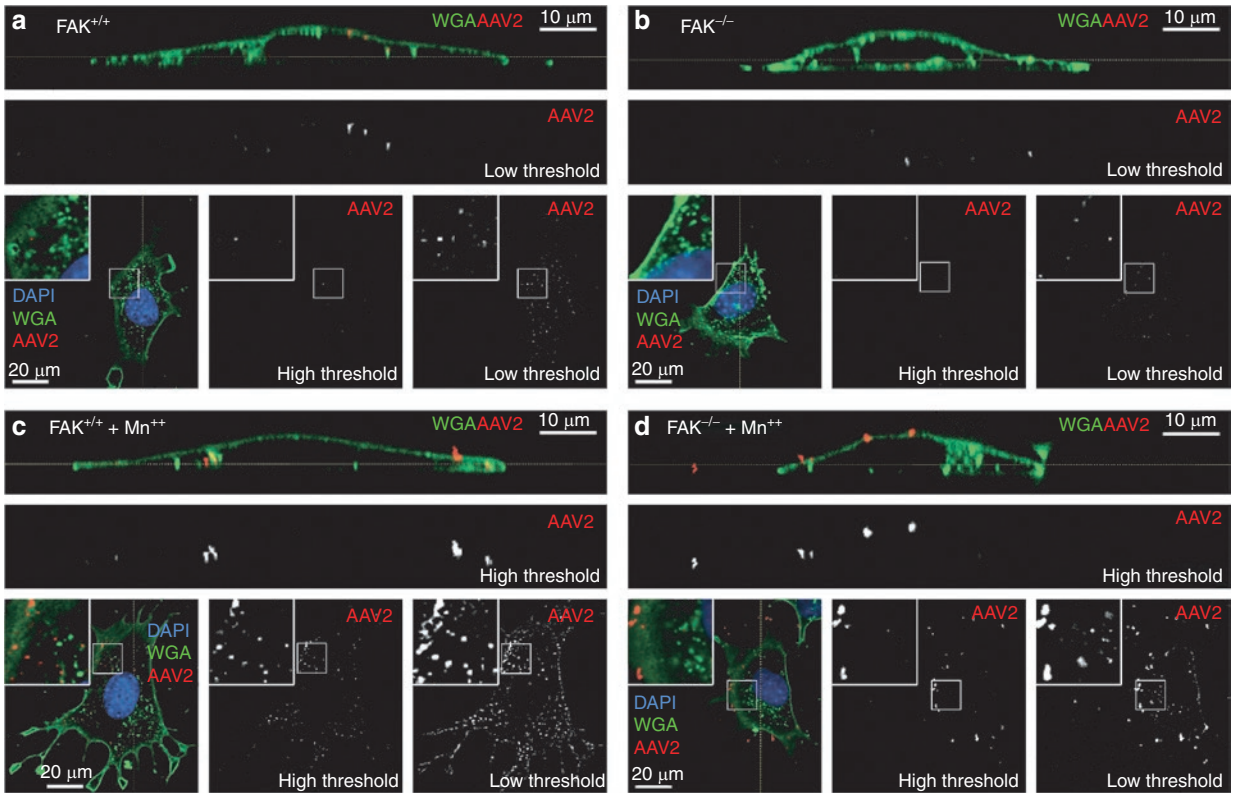

Figure 5 Mn^{++} promotes adeno-associated virus (AAV) clustering independently of focal adhesion kinase (FAK). (**a–d**) FAK$^{+/+}$ and FAK$^{-/-}$ mouse embryonic fibroblasts (MEFs) were infected with Alexa568-recombinant adeno-associated virus 2 (rAAV2) in the (**a**, **b**) absence and (**c**, **d**) presence of Mn^{++} for 1 hour. Membranes were stained with AlexaFluor-488 Wheat Germ Agglutinin (Alexa488-WGA) to demark the plasma membrane and endosomes. A series of XY confocal images were taken through each cell (square images at the bottom of each panel) and a reconstructed YZ-vertical image was created using metamorph software (top rectangular panels) to help demonstrate the location of AAV objects relative to the plasma membrane. The location of the XY slice (square panels) is marked on the YZ panels by a yellow line. Similarly the location of the YZ slice (rectangular panels) is marked on the XY panels by a yellow line. AAV single channel images are depicted at both high and low threshold to demonstrate increased cluster size and intensity in the presence of Mn^{++} (**c**, **d**). The boxed regions in square panels are enlarged as an inset.

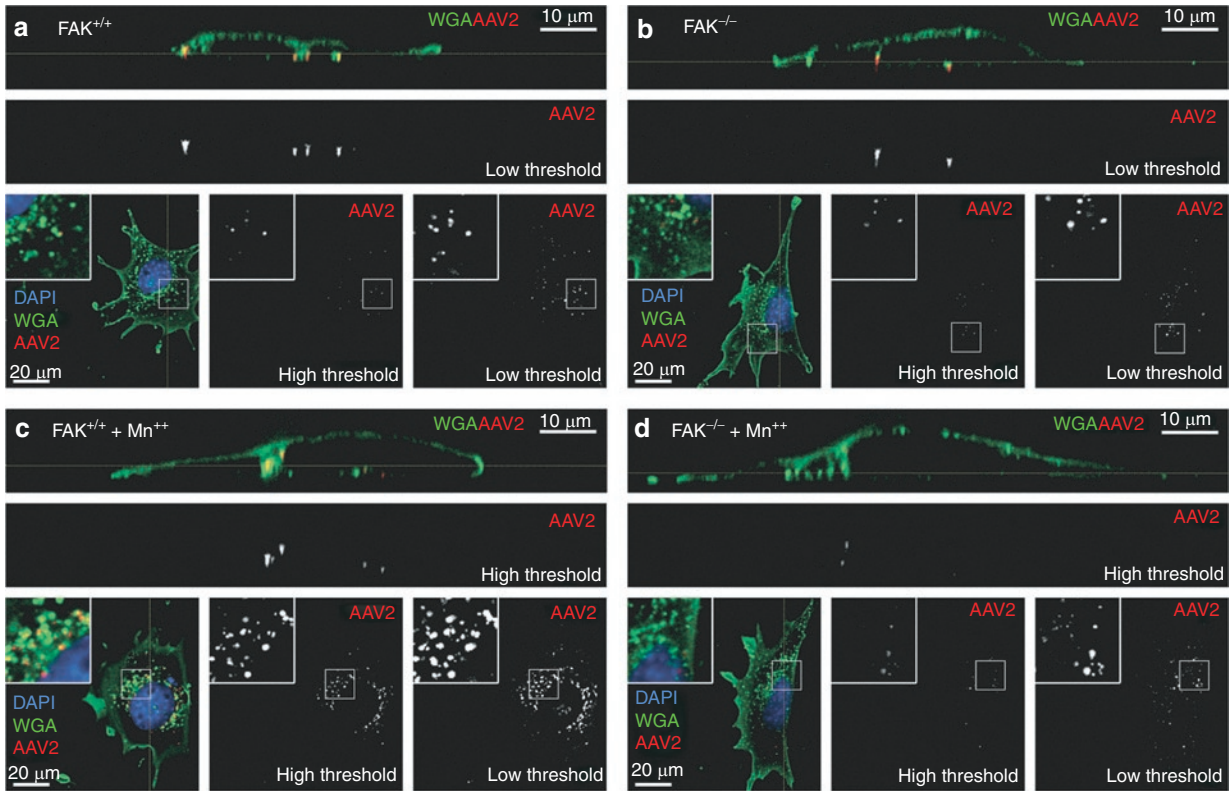

Figure 6 Focal adhesion kinase (FAK) is required for the internalization of Mn^{++} induced adeno-associated virus (AAV) aggregates. (**a**–**d**) FAK$^{+/+}$ and FAK$^{-/-}$ mouse embryonic fibroblasts (MEFs) were infected with Alexa568-recombinant adeno-associated virus 2 (rAAV2) in the (**a**, **b**) absence and (**c**, **d**) presence of Mn^{++} for 2 hours in the presence of Mn^{++}, followed by 2 hours in virus- and Mn^{++}-free media. Membranes were stained with AlexaFluor-488 Wheat Germ Agglutinin (Alexa488-WGA) to demark the plasma membrane and endosomes. A series of XY confocal images were taken through each cell (square images at the bottom of each panel) and a reconstructed YZ-vertical image was created using metamorph software (top rectangular panels) to help demonstrate the location of AAV objects relative to the plasma membrane. The location of the XY slice (square panels) is marked on the YZ panels by a yellow line. Similarly the location of the YZ slice (rectangular panels) is marked on the XY panels by a yellow line. AAV single channel images are depicted at both high and low threshold to demonstrate increased cluster size and intensity in the presence of Mn^{++} (**c**, **d**). In the absence of Mn^{++}, rAAV2 is internalized regardless of FAK expression (**a**, **b**). In the presence of Mn^{++}, FAK competent (**c**) cells internalize the large and bright AAV clusters, however, in FAK$^{-/-}$ MEFs these rAAV2 clusters are either broken apart or remain associated with the cell surface (**d**). The boxed regions in square panels are enlarged as an inset.

Membranes were marked with Alexa488-labeled wheat germ agglutinin (Alexa488-WGA) to help differentiate intracellular and surface-bound rAAV2. Similarly to PMEFs, treatment with Mn^{++} induced clustering of rAAV2 in both FAK competent and knockout cells (**Figure 5a–d**) after 1 hour of infection, suggesting that clustering of AAV2 on activated integrins is independent of FAK. By 4 hours following infection, FAK$^{+/+}$ MEFs internalized many more concentrated clusters of rAAV2 in the presence of Mn^{++}, as compared to FAK$^{-/-}$ MEFs in the presence of Mn^{++} (**Figure 6a–d**). Interestingly, very few bright clusters of AAV remained on the surface of FAK$^{-/-}$ MEFs in the presence of Mn^{++} by 4 hours, suggesting that the rAAV2/integrin aggregates are ultimately broken up and internalized by a FAK-independent mechanism since transduction and viral uptake of FAK null cells is equivalent with or without Mn^{++} (**Figure 4a,d**).

The integrin-linked pathway mediates highly efficient AAV1 and AAV6, but not AAV5, transduction

The interaction between AAV2 and α5β1 integrin was previously mapped to an NGR sequence in the capsid protein VP3.[6] Although NGR is not an efficient integrin ligand, both asparagine and aspartic acid undergo nonenzymatic deamination to form isoaspartic acid–glycine–arginine (IsoDGR), which is an efficient integrin ligand. An alignment of AAV capsid proteins reveals that the NGR or DGR sequence is highly conserved among many serotypes of AAV (**Supplementary Table S1**), with the notable exceptions of AAV5 and 11. Interestingly, AAV5 and AAV11 are among the least conserved of the AAV serotypes.[31] If indeed NGR and DGR capsid sequence conservation predicts the ability of various rAAV serotypes to interact with integrins, we expected that serotypes with these sequences would be responsive to enhancements in transduction in the presence of Mn^{++}. To test this hypothesis, we evaluated Mn^{++}-induced transduction with rAAV1 and rAAV6 (both containing NGR sequences) and rAAV5 (containing an EGA sequence). As predicted, Mn^{++} treatment for 2 hours at the time of infection increased transduction of rAAV1 (11-fold) and rAAV6 (16-fold), but only slightly enhanced rAAV5 transduction (twofold) (**Figure 7**). These findings provide further support for our model that integrin-activation at the cell surface is a rate-limiting step for highly productive transduction of fibroblasts by multiple serotypes containing NGR sequences in their capsid.

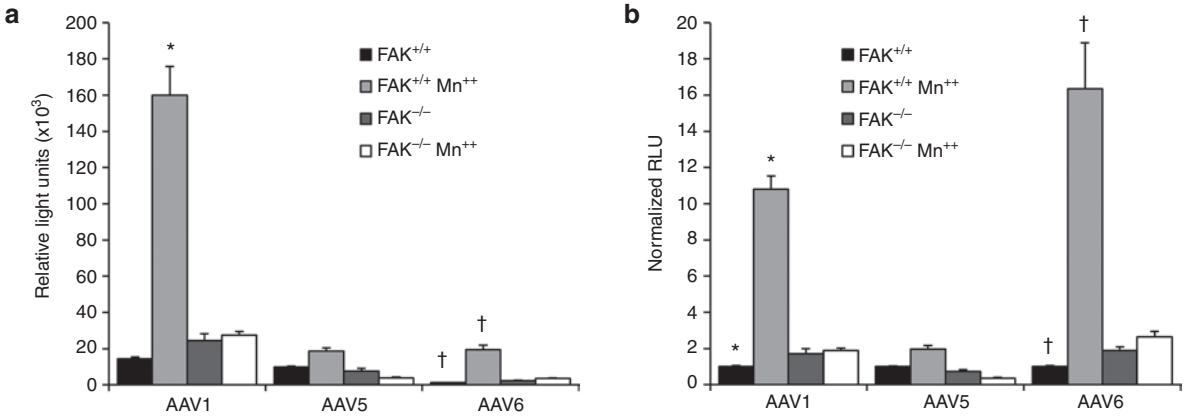

Figure 7 Mn++-induced integrin activation enhances transduction by AAV1 and AAV6, but not AAV5. (**a**) FAK$^{+/+}$ and FAK$^{-/-}$ mouse embryonic fibroblasts (MEFs) were infected with AAV serotypes 1, 5, and 6 containing the identical luciferase reporter in the presence and absence of Mn++. The relative luciferase activity at 24 hours postinfection is plotted for each serotype. Treatment with Mn++ increased transduction of integrin-binding domain-containing serotypes AAV1 and AAV6 only in of FAK$^{+/+}$ competent MEFs (AAV1 10.8-fold and AAV6 16.3-fold). AAV5, which lacks a theoretical integrin-binding domain, was only slightly induced (twofold) by Mn++ treatment at the time of infection. (**b**) Transduction data in panel A was normalized to untreated FAK$^{+/+}$ for each AAV serotype. Values represent the mean ± SEM for $N = 18$ independent infections. *, †mark significant differences as assessed by a two-tailed Student's *t*-test ($P < 0.0001$).

DISCUSSION

As the use of AAV vectors in clinical trials continues to grow, there is an increasing need to better understand the biology of rAAV transduction and the factors that limit its efficacy. It is clear from previous studies that the extent of rAAV internalization does not predict efficiency of expression of an encoded transgene. It has been hypothesized that a large number of entry pathways are available of rAAV, but it remains unclear what pathways of entry are most efficient from a transduction standpoint. In the present study, we demonstrate that there is coreceptor competition for the endocytosis of AAV2 into fibroblasts and that selective activation of integrins enhances endocytosis through a FAK-dependent pathway that is highly efficient for transduction.

Previous studies have demonstrated that AAV binding and endocytosis are separate events mediated by primary binding receptors (HSPG and sialic acids) and a variety of coreceptors, including several integrins. Our studies suggest that coreceptors present on the plasma membrane compete for a limited quantity of surface-bound AAV. Although the precise identity of AAV2-binding receptor(s) remains unknown, it is clear that the quantity of AAV2 available for endocytosis is dependent on the primary binding receptor and remains unchanged by treatment with Mn++ or the presence of FAK.

Our fluorescent imaging studies demonstrate that Mn++ promotes increased clustering of surface-bound AAV2 at sites of integrin activation (*i.e.*, vinculin recruitment). Furthermore, this Mn++-induced AAV2 clustering and transduction was inhibited by RDGS peptide. Importantly, we did not observe AAV2 in vinculin-containing focal adhesions, as the binding site of these integrins is already occupied by ligands from the extracellular matrix. A variety of integrins of the RGD-binding class mediate similar endocytic pathways, which vary with expression in each tissue. For example, HeLa cells rely on αVβ5 integrins[7] while α5β1 integrin is the preferred receptor in HEK 293 cells.[6] Consistent with models of integrin signaling, we propose that the cytosolic machinery used during integrin-mediated endocytosis of AAV2 and trafficking through the endosomal compartment en route to the nucleus is highly conserved. However, we also propose that there must be a fundamental difference between integrin signaling that promotes endocytosis as opposed to focal adhesion formation. Integrins are internalized through either caveolin- or clathrin-mediated endocytosis and are impacted by a variety of factors, including cell division, cell migration, subcellular integrin distribution, and signaling through associated receptor proteins.[32] After traveling to the sorting endosome, integrins can be recycled to the surface of the cell by at least four distinct pathways or sent to the lysosome via the late endosome for degradation.[32] This suggests that the endosomal fate of AAV may be coupled to more than just the coreceptor that initiates endocytosis—for example the local environment of the coreceptor. Although the role of FAK in recycling and turnover of integrins is not well established, our results suggest that FAK is critical for endocytosis of rAAV2 following integrin activation. Furthermore, under conditions where integrin activation is enhanced (*i.e.*, with Mn++), both α5 integrin and vinculin appeared to stay associated with endosomes-containing rAAV2 at least during the initial phases of trafficking.

Our studies demonstrate that FAK is necessary for Mn++-dependent enhancements in transduction of fibroblasts by rAAV2, rAAV1 and rAAV6, implicate integrins as important entry portals for each of these serotypes. Mn++ treatment promotes integrin-dependent rAAV2 clustering at the plasma membrane independently of FAK; however, internalization of these larger clusters appears to require FAK. The finding that integrin/FAK-dependent endocytosis incorporates significantly greater rAAV into each endosome could have important implications on subsequent steps, particularly endosomal escape. For example, the efficiency of endosomal escape could be greater when clusters of virions are contained within the endosome—potentially due to cooperative action of capsid proteins on endosome lysis.

These observations support a basic model of proximal events during AAV infection required for efficient transduction (**Figure 8**). After binding to a primary receptor (*i.e.*, HSPG being

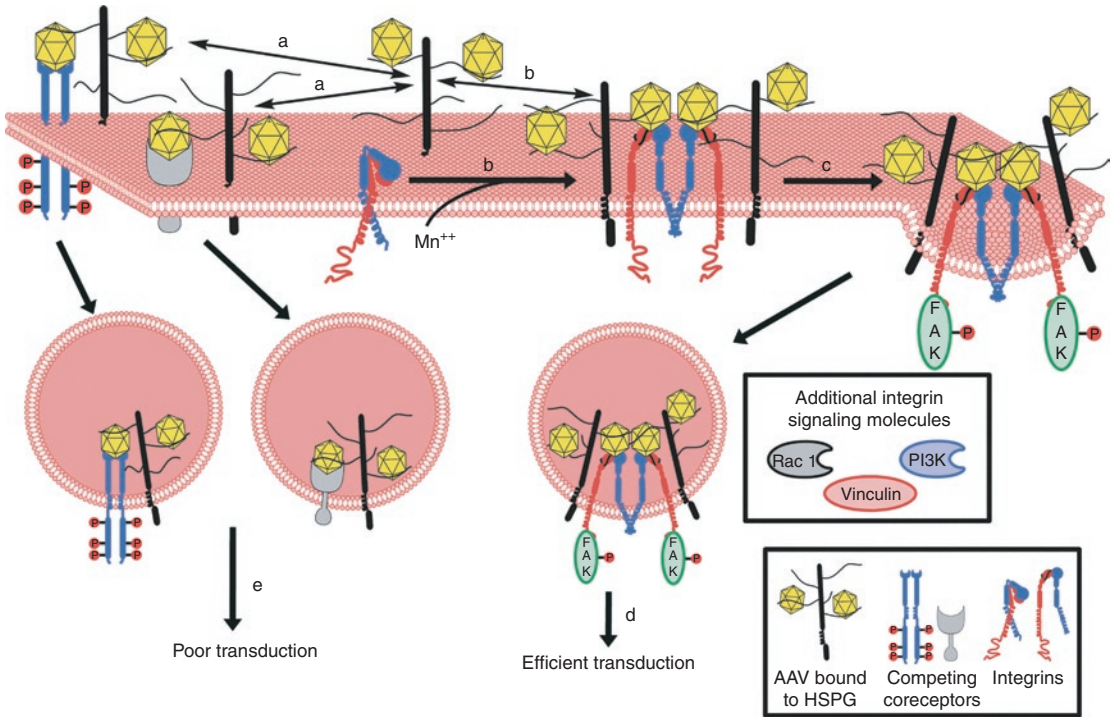

Figure 8 Model for coreceptor competition of heparan sulfate proteoglycan (HSPG)-bound AAV2 and molecular signaling initiated after integrin activation. (**a**) After binding to primary receptors (*i.e.*, HSPG for AAV2), coreceptors compete to internalize HSPG-bound AAV2. (**b**) Treatment with Mn++ partially activates integrins, facilitating AAV2–integrin interactions and clustering on the cell surface, thereby increasing the quantity of AAV2 ultimately internalized by integrin-mediated endocytosis. These complexes likely consist of many integrins and HSPG/AAV2 complexes, although only two are shown. (**c**) These integrin complexes then recruit intracellular FAK and other effectors such as vinculin, phosphatidylinositol-3 kinase (PI3K), Rac1 to initiate endocytosis of the integrin-linked AAV2 complexes. (**d**) Following endocytosis, integrin-linked pathways undergo efficient intracellular processing, which lead to highly efficient transduction (*i.e.*, expression of the encoded transgene). (**e**) By contrast, competing AAV2 internalization by nonintegrin coreceptors leads to much less efficient intracellular processing and transduction.

a major one for AAV2), coreceptors, including integrins, compete for a finite quantity of bound AAV (**Figure 8a**). The identity of the coreceptors, their distribution relative to the binding receptor, and the relative expression of each, likely determining how much AAV is internalized by each coreceptor. Such factors almost certainly vary between tissues. Treatment with Mn++ partially activates integrins, thereby promoting AAV–integrin interactions and resulting in the large clusters of AAV observed on the surface of cells (**Figure 8b**). These integrin aggregates then recruit a variety of signaling molecules, including FAK and vinculin, which in turn, initiate endocytosis of the protein complex (**Figure 8c**). rAAV that is internalized by integrin-mediated endocytosis appears to be processed much more efficiently within the cell since it gives rise to much higher levels of transgene expression (**Figure 8e**). By contrast, virus internalized by competing coreceptor pathways is processed inefficiently within the cell and lead to low levels of transgene expression (**Figure 8e**).

Active integrins recruit FAK, which is reported to undergo intermolecular autophosphorylation and initiate Rac1 and PI3K signaling—two factors also shown to be required for efficient rAAV2 endocytosis[7]—and this results in the endocytosis of Mn++-induced AAV2 clusters (**Figure 8c**). Previous studies on FAK signaling demonstrate that c-Src is recruited to activated FAK during the course of focal adhesion formation and this step is required for additional downstream signaling event.[18,27] Consistent with a role of c-Src in FAK signaling, rAAV2 transduction of MEFs lacking the Src family homologues c-Src, Yes, and Fyn (SYF cells) was ~2,900 times less than c-Src complimented SYF MEFs (SYF cells-expressing recombinant c-Src) (**Supplementary Figure S3**). This finding establishes c-Src as an additional effector of the integrin/FAK pathway required for efficient rAAV2 transduction.

Although manganese is likely not compatible with *in vivo* use, these studies suggest that methods of enhancing integrin-mediated endocytosis of rAAV serotypes containing integrin-ligand binding domains could substantially increase their efficacy for gene therapy. In support of this concept, incorporation of RGD-containing peptide into the rAAV2 capsid that are more readily accessible for integrin interactions have been shown to enhance rAAV transduction independent of HSPG.[25] This concept of promoting AAV-integrin interactions may prove invaluable to increasing AAV transduction efficiency in a wide range of tissues. Another potential approach to increase the fraction of AAV that is internalized by integrins would be to block alternative coreceptors and/or endocytic pathways that are less efficient in delivering AAV to the nucleus.

In summary, promoting AAV–integrin interactions with Mn++ can increase the fraction of surface-bound rAAV2 internalized by integrin-mediated endocytosis. Our data suggests that rAAV2 interaction with integrins initiates clustering and subsequent recruitment of intracellular vinculin and FAK, which in turn, induces signaling necessary for endocytosis. Similar to other models of integrin signaling, FAK recruitment of Rac1, PI3K, and

c-Src likely also facilitate the molecular signals necessary for successful and efficiency navigation of virion-containing endosomes to the nucleus.

MATERIALS AND METHODS

Cells, plasmids, and AAV vectors. PMEFs were isolated from a wild-type C57B6 mouse (PMEF). FAK$^{+/+}$ and FAK$^{-/-}$ MEF were obtained from the ATCC (Manassas, VA); these cells were isolated from E8.0 day mouse embryo of littermate-matched p53$^{-/-}$ mice. The Src family kinase knockout MEFs (Src$^{-/-}$, Yes$^{-/-}$, Fyn$^{-/-}$; called SYF) and the SYF cells stably expressing c-Src (Src$^{-/-}$, Yes$^{-/-}$, Fyn$^{-/-}$ + c-Src; called SYF + c-Src) were obtained from the ATCC and were derived from 9-day old embryonic fibroblasts and immortalized with SV40 antigen. All cells were grown in Dulbecco's modified Eagle's media (DMEM) supplemented with 10% fetal bovine serum and penicillin/streptomycin. An enhanced GFP tagged α5-integrin-receptor construct (ITGA5-GFP) was obtained from AddGene (15238) and was originally made by Dr Louis Reichardt. All AAV vectors used encode CMV-luciferase flanked by the AAV2 inverted terminal repeats and the capsid proteins from the indicated serotype. rAAV1, rAAV2, rAAV5, and rAAV6 were generated using a triple plasmid transfection method and purification protocols previously described by our laboratory.[33]

rAAV-luciferase transduction assay. Fibroblasts and HeLa cells were seeded (2×10^5 HeLa cells/well; 10^5 PMEFs, FAK MEFs, or SYF MEFs/well) on rat collagen I coated 24-well plates (BD BioCoat, Franklin Lakes, NJ) and cultured for 24 hours. Media was then removed and replaced with 500 µl of DMEM containing rAAV (2×10^8 particles/well) with or without 0.7 mmol/l Manganese(II) chloride tetrahydrate (Mn^{++}; Sigma, St Louis, MO), 1 mg/l heparin sodium salt (heparin; Sigma), 100 µg/ml RGDS (Abbiotec, San Diego, CA), and 1 µmol/l PF-00562271 (FAK inhibitor; Selleck Chemicals, Houston, TX). After 2 hours the media was replaced with standard culture media without Mn^{++} or virus for 22 hours. Transduction was quantified using a luciferase reporter assay (Promega, Madison, WI) according to the manufacturer's instructions.

Transduction of prebound AAV2-luciferase. Cells were seeded on collagen-coated 24 well plates as described above. Before infection, cells were shifted to 12 °C for 20 minutes to prevent endocytosis. Media was then exchanged for DMEM containing AAV2-luciferase without Mn^{++} for 1 hour at 12 °C. Cells were then washed with warm DMEM and incubated at 37 °C for 2 hours in DMEM supplemented with or without Mn^{++} (0.7 mmol/l). The media was then exchanged to remove Mn^{++} and the luciferase assay was carried out as described as above at 24 hours postinfection.

Quantification of cell-associated and internalized AAV2 particles. Fibroblasts and HeLa cells were seeded (10^6 HeLa cells/well; 5×10^5 FAK MEFs/well) on rat collagen I coated 6-well plates (BD BioCoat) and incubated for 24 hours. Wells were then washed with DMEM followed by infection with rAAV-luciferase (10^9 particles/well) in 1 ml of DMEM with or without 0.7 mmol/l Mn^{++}. Cells were trypsinized to remove surface-bound AAV, spun at 3,000*g*, and washed three times in phosphate-buffered saline (PBS). The cell pellet was lysed in 400 µl of Promega luciferase reporter assay lysis buffer and diluted with 1.2 ml PBS. Samples were then boiled and cleared at 1,000*g* and viral genomes in the supernatant were quantified by TaqMan real-time PCR as previously described by our laboratory.[14] To evaluate both cell-associated membrane-bound and internalized virus, cells were directly lysed on the plates after washing before PCR assays for viral genomes.

Labeling AAV2 with Alexa568. AAV2-luciferase was dialyzed to PBS overnight and labeled with Alexa Fluor 568 protein labeling kit (Invitrogen, Grand Island, NY; A-10238) according to methods previously described by our laboratory (Alexa568-rAAV2).[34]

Quantification of AAV2 clustering. C57B6 PMEFs were infected at 37 °C with 100 µl of DMEM containing Alexa568-rAAV2 (20,000 particles/cell) with or without Mn^{++} (0.7 mmol/l) for 60 minutes. Samples were then washed three times with PBS to remove unbound virus and fixed in 4% paraformaldehyde for 15 minutes. After washing four times in PBS, samples were permeabilized in PBS containing 5% donkey serum, 0.5% bovine serum albumin fraction 5, and 0.1% Triton-X100, washed four times with PBS, and covered in DAPI mounting media (Vectashield H-1200; Vectashield, Burlingame, CA). Metamorph software was then used to 3D deconvolute images and quantify the size and integrated intensity of AAV aggregates.

Analysis of α5 integrin recruitment. C57B6 PMEF were transfected by electroporation with GFP tagged α5 integrin (ITGA5-GFP) and plated (2×10^5) 2 days later on 35-mm glass bottom dishes (MatTek, Ashland, MA). Cells were then infected for 1 hour with Alexa568-rAAV2 and then fixed and mounted as above. To evaluate AAV2 and α5 integrin colocalization, images through the middle of the cell were taken on a Zeiss LSM 700 confocal microscope and processed using Metamorph 3D software.

Analysis of vinculin recruitment. C57B6 PMEF (2×10^5) plated on 35-mm glass bottom dishes were washed with DMEM and infected with Alexa-labeled AAV2 as described above for 60 minutes. After washing, fixing, and blocking in PBS containing 5% donkey serum and 0.5% bovine serum albumin, samples were then stained with a mouse monoclonal anti-vinculin antibody (Sigma; V9131) in 0.5% bovine serum albumin, 0.1% triton X-100 in PBS (1:500) for overnight at 4 °C. Lastly, samples were washed four times in PBS, stained with an Alexa Fluor 488 anti-mouse secondary (Invitrogen; A21202) for 1 hour at room temperature, washed four times with PBS, and covered in mounting media with DAPI. Images were captured as confocal slices through the cell as indicated to demonstrate the degree of colocalization of vinculin with Alexa568-AAV2 at focal adhesions and the plasma membrane, respectively.

Analysis of FAK-dependence on AAV2 internalization. FAK$^{+/+}$ and FAK$^{-/-}$ MEF (2×10^5) plated on 35-mm glass bottom dishes (MatTek) were washed with DMEM and the center insert was covered with 100 µl of serum-free DMEM containing Alexa568-AAV2 (20,000 particles/cell) with or without Mn^{++} (0.7 mmol/l). Infections were performed for either 1 hour in the continuous presence of Mn^{++} or for 2 hours in the presence of Mn^{++} followed by a 2-hour chase without Mn^{++} in the presence of 10% serum-containing media. Samples were then washed three times with PBS to remove unbound virus and fixed in 4% paraformaldehyde for 1 hour. After washing four times in PBS, membranes and endosomes-containing sialic acid or *N*-acetylglucosaminyl sugar residues were labeled with AlexaFluor-488 conjugated wheat germ agglutinin (Alexa488-WGA; Invitrogen, W11261) for 1 hour. Samples were then washed four times in PBS and blocked and mounted as described above for analysis by confocal microscopy.

SUPPLEMENTARY MATERIAL

Table S1. The theoretical integrin ligands NGR and DGR in AAV caspids are highly conserved across serotypes.
Figure S1. Retention of surface-bound AAV2 is not altered by Mn^{++}.
Figure S2. Heparin inhibits AAV2 transduction of Mn^{++} treated MEFs.
Figure S3. Src tyrosine kinase is required for efficient AAV2 transduction of MEFs.

ACKNOWLEDGMENTS

This work was supported by NIH grants HL108902 (to J.F.E.), F30HL103147 (to P.M.K.), the Roy J. Carver Chair in Molecular Medicine (to J.F.E.), and the University of Iowa Center for Gene Therapy (DK54759).

REFERENCES

1. Seiler, MP, Miller, AD, Zabner, J and Halbert, CL (2006). Adeno-associated virus types 5 and 6 use distinct receptors for cell entry. *Hum Gene Ther* **17**: 10–19.
2. Kern, A, Schmidt, K, Leder, C, Müller, OJ, Wobus, CE, Bettinger, K *et al.* (2003). Identification of a heparin-binding motif on adeno-associated virus type 2 capsids. *J Virol* **77**: 11072–11081.

3. Summerford, C and Samulski, RJ (1998). Membrane-associated heparan sulfate proteoglycan is a receptor for adeno-associated virus type 2 virions. *J Virol* **72**: 1438–1445.
4. Ng, R, Govindasamy, L, Gurda, BL, McKenna, R, Kozyreva, OG, Samulski, RJ *et al.* (2010). Structural characterization of the dual glycan binding adeno-associated virus serotype 6. *J Virol* **84**: 12945–12957.
5. Wu, Z, Miller, E, Agbandje-McKenna, M and Samulski, RJ (2006). Alpha2,3 and alpha2,6 N-linked sialic acids facilitate efficient binding and transduction by adeno-associated virus types 1 and 6. *J Virol* **80**: 9093–9103.
6. Asokan, A, Hamra, JB, Govindasamy, L, Agbandje-McKenna, M and Samulski, RJ (2006). Adeno-associated virus type 2 contains an integrin alpha5beta1 binding domain essential for viral cell entry. *J Virol* **80**: 8961–8969.
7. Sanlioglu, S, Benson, PK, Yang, J, Atkinson, EM, Reynolds, T and Engelhardt, JF (2000). Endocytosis and nuclear trafficking of adeno-associated virus type 2 are controlled by rac1 and phosphatidylinositol-3 kinase activation. *J Virol* **74**: 9184–9196.
8. Qing, K, Mah, C, Hansen, J, Zhou, S, Dwarki, V and Srivastava, A (1999). Human fibroblast growth factor receptor 1 is a co-receptor for infection by adeno-associated virus 2. *Nat Med* **5**: 71–77.
9. Akache, B, Grimm, D, Pandey, K, Yant, SR, Xu, H and Kay, MA (2006). The 37/67-kilodalton laminin receptor is a receptor for adeno-associated virus serotypes 8, 2, 3, and 9. *J Virol* **80**: 9831–9836.
10. Kashiwakura, Y, Tamayose, K, Iwabuchi, K, Hirai, Y, Shimada, T, Matsumoto, K *et al.* (2005). Hepatocyte growth factor receptor is a coreceptor for adeno-associated virus type 2 infection. *J Virol* **79**: 609–614.
11. Kurzeder, C, Koppold, B, Sauer, G, Pabst, S, Kreienberg, R and Deissler, H (2007). CD9 promotes adeno-associated virus type 2 infection of mammary carcinoma cells with low cell surface expression of heparan sulphate proteoglycans. *Int J Mol Med* **19**: 325–333.
12. Ding, W, Zhang, L, Yan, Z and Engelhardt, JF (2005). Intracellular trafficking of adeno-associated viral vectors. *Gene Ther* **12**: 873–880.
13. Duan, D, Yue, Y, Yan, Z, Yang, J and Engelhardt, JF (2000). Endosomal processing limits gene transfer to polarized airway epithelia by adeno-associated virus. *J Clin Invest* **105**: 1573–1587.
14. Yan, Z, Lei-Butters, DC, Liu, X, Zhang, Y, Zhang, L, Luo, M *et al.* (2006). Unique biologic properties of recombinant AAV1 transduction in polarized human airway epithelia. *J Biol Chem* **281**: 29684–29692.
15. Curnis, F, Longhi, R, Crippa, L, Cattaneo, A, Dondossola, E, Bachi, A *et al.* (2006). Spontaneous formation of L-isoaspartate and gain of function in fibronectin. *J Biol Chem* **281**: 36466–36476.
16. Koivunen, E, Gay, DA and Ruoslahti, E (1993). Selection of peptides binding to the alpha 5 beta 1 integrin from phage display library. *J Biol Chem* **268**: 20205–20210.
17. Spitaleri, A, Mari, S, Curnis, F, Traversari, C, Longhi, R, Bordignon, C *et al.* (2008). Structural basis for the interaction of isoDGR with the RGD-binding site of alphavbeta3 integrin. *J Biol Chem* **283**: 19757–19768.
18. Cohen, LA and Guan, JL (2005). Mechanisms of focal adhesion kinase regulation. *Curr Cancer Drug Targets* **5**: 629–643.
19. Kallergi, G, Agelaki, S, Markomanolaki, H, Georgoulias, V and Stournaras, C (2007). Activation of FAK/PI3K/Rac1 signaling controls actin reorganization and inhibits cell motility in human cancer cells. *Cell Physiol Biochem* **20**: 977–986.
20. Tomar, A and Schlaepfer, DD (2009). Focal adhesion kinase: switching between GAPs and GEFs in the regulation of cell motility. *Curr Opin Cell Biol* **21**: 676–683.
21. Harburger, DS and Calderwood, DA (2009). Integrin signalling at a glance. *J Cell Sci* **122**(Pt 2): 159–163.
22. Luo, BH, Carman, CV and Springer, TA (2007). Structural basis of integrin regulation and signaling. *Annu Rev Immunol* **25**: 619–647.
23. Banno, A and Ginsberg, MH (2008). Integrin activation. *Biochem Soc Trans* **36**(Pt 2): 229–234.
24. Takagi, J, Petre, BM, Walz, T and Springer, TA (2002). Global conformational rearrangements in integrin extracellular domains in outside-in and inside-out signaling. *Cell* **110**: 599–511.
25. Shi, W and Bartlett, JS (2003). RGD inclusion in VP3 provides adeno-associated virus type 2 (AAV2)-based vectors with a heparan sulfate-independent cell entry mechanism. *Mol Ther* **7**: 515–525.
26. Xiong, JP, Stehle, T, Zhang, R, Joachimiak, A, Frech, M, Goodman, SL *et al.* (2002). Crystal structure of the extracellular segment of integrin alpha Vbeta3 in complex with an Arg-Gly-Asp ligand. *Science* **296**: 151–155.
27. Cary, LA and Guan, JL (1999). Focal adhesion kinase in integrin-mediated signaling. *Front Biosci* **4**: D102–D113.
28. Mierke, CT (2009). The role of vinculin in the regulation of the mechanical properties of cells. *Cell Biochem Biophys* **53**: 115–126.
29. Hansen, J, Qing, K and Srivastava, A (2001). Adeno-associated virus type 2-mediated gene transfer: altered endocytic processing enhances transduction efficiency in murine fibroblasts. *J Virol* **75**: 4080–4090.
30. Chiquet, M, Gelman, L, Lutz, R and Maier, S (2009). From mechanotransduction to extracellular matrix gene expression in fibroblasts. *Biochim Biophys Acta* **1793**: 911–920.
31. Gao, G, Vandenberghe, LH and Wilson, JM (2005). New recombinant serotypes of AAV vectors. *Curr Gene Ther* **5**: 285–297.
32. Caswell, PT, Vadrevu, S and Norman, JC (2009). Integrins: masters and slaves of endocytic transport. *Nat Rev Mol Cell Biol* **10**: 843–853.
33. Yan, Z, Zak, R, Luxton, GW, Ritchie, TC, Bantel-Schaal, U and Engelhardt, JF (2002). Ubiquitination of both adeno-associated virus type 2 and 5 capsid proteins affects the transduction efficiency of recombinant vectors. *J Virol* **76**: 2043–2053.
34. Keiser, NW, Yan, Z, Zhang, Y, Lei-Butters, DC, and Engelhardt, JF (2011). Unique Characteristics of AAV1, 2, and 5 Viral Entry, Intracellular Trafficking, and Nuclear Import Define Transduction Efficiency in HeLa Cells.*Hum Gene Ther* **22**:1433–1444.